

# Correlation Between Interfacial Free Energy and Albumin Adsorption in Poly(acrylonitrile–acrylamide–acrylic acid) Hydrogels

DAVID SHIAW-GUANG HU\* and CHUEN-EN TSAI

Program in Polymers and Textiles, Department of Textile Engineering, National Taiwan Institute of Technology, Taipei, Taiwan 10772, Republic of China

## SYNOPSIS

An investigation on the influence of chemical compositions and surface properties (e.g., surface free energy in air and hydrogel–water interfacial energy) on the adsorption of bovine serum albumin (BSA) at pH 7.4 on to a series of poly(acrylonitrile–acrylamide–acrylic acid) hydrogels was carried out. The interfacial energetics were determined from the contact angle data for air–gel and octane–gel in the water environment and the specific adsorption of BSA was determined with UV–VIS spectroscopy. It is shown that the higher contents of amide and acid groups in hydrogel bulk lead to the greater polar component of surface energy in air and the greater BSA adsorption in aqueous solutions. The BSA adsorption decreases with water amount in gels at lower amide/acid contents and increases at higher contents. The results imply that the interfacial interactions between the protein and the reorganized hydrogel interface in exposure with water, as well as the penetration of protein into pores of swollen gels, influence the BSA adsorption. © 1996 John Wiley & Sons, Inc.

## INTRODUCTION

Surface and interfacial behavior of biomedical polymers in the aqueous environment play a distinct role in determining the material biocompatibility with the living body. Specifically, the interfacial free energy, surface morphology, electric potential at surface, etc., of polymers are crucial to the dynamics occurring in the medical and biotechnological systems. A class of water-filling polymeric biomaterials, namely hydrogels, consists of swollen interpenetrating polymer networks and neutral and ionic hydrophiles. Hydrogels are well known for their low interfacial energy in contact with bulk water, limited protein adsorption onto them, and excellent biocompatibility.<sup>1</sup> Recently, polyelectrolyte gels responsive to environmental stimuli such as temperature, pH, composition of solution in contact, light, and electric current have received much attention in the category of hydrogels research. This class of

“intelligent” polymers may be applied to chemo-mechanical energy conversion devices, artificial muscles, and self-regulated drug delivery systems.<sup>2</sup> In addition, these temperature- and pH-sensitive gels have been studied for separation of proteins during phase transition of gels,<sup>3</sup> in which the modulation of material compositions and subsequent interfacial properties should be taken into account to reduce the excess protein attachment to gels functioning as separation media. Since gels consist of substantial amount of water, it is advisable to understand the role of water in the interfacial energetics of hydrogels.

The higher water content in non-ionic hydrogels was found to lead to lower interfacial free energy in water and greater polar component of surface tension of hydrogels.<sup>4</sup> Ko and colleagues<sup>5</sup> investigated the wettability of hydroxyethyl methacrylate (HEMA)- and ethylmethacrylate (EMA)-grafted polyethylene using the contact angle of liquid drops in the air and water environments, and found that the polar component of interfacial energy of hydrogels in water and critical surface tension increased with the amount of hydrophilic HEMA.

\* To whom correspondence should be addressed.

For ionic poly(2-hydroxyethyl methacrylate/methacrylic acid) (P(HEMA/MAA)) copolymer gels, various proteins such as  $\gamma$ -globulin, albumin, fibrinogen, etc., are adsorbed onto gels so that the MAA moieties promote the protein adsorption at pH 7.4.<sup>6,7</sup> Infrared (IR) analysis revealed hydrogen bonding between hydroxyls of gels and imines (NH) of mucin and ionic bonding between carboxyls in MAA-containing gels and amine in mucin, leading to irreversible protein adsorption.<sup>8</sup> A study of several plasma proteins (i.e., albumin,  $\gamma$ -globulin, and fibrinogen) on polystyrene/PHEMA block copolymers by Sakurai and coworkers showed that proteins were preferentially adsorbed onto hydrophilic or hydrophobic domains.<sup>9</sup> The surface roughness and microporosity of gels are believed to enhance the protein adsorption,<sup>10</sup> in contrast to the gels with smooth surface.

However, to our knowledge, the literature seems to have not reported the relationships between the interfacial energy and protein adsorption for ionic multicomponent hydrogels. We have recently studied the thermodynamics, volume phase transition, and relaxation transitions in poly(acrylonitrile-acrylamide-acrylic acid), abbreviated P(AN-AAm-AA), multicomponent hydrogels. Previous studies in this series have been concerned with the relationships between the dynamic dielectric properties and water absorption, as well as the states of water and critical phenomena of these gels.<sup>11,12</sup> In this series of materials, the amount of bound water is an increasing function of acid or amide content, and the amount of unbound water has a minimum at a certain acid/amide content.

This study is aimed at investigating the role of water in interfacial free energy of P(AN-AAm-AA) hydrogels and correlating the above surface/interfacial properties with the adsorption of bovine serum albumin (BSA) onto these structurally complex gels. The effect of small amounts (say, less than 5 mol % of monomer units in a polymer chain) of ionizable moieties on polymer chains, i.e.,  $-\text{COOH}$ , on the protein deposition on hydrogels, will also be assessed.

## EXPERIMENTAL

### Preparation and Characterization of Gels

Gels were prepared sequentially through the reaction of polyacrylonitrile (Aldrich, number-average molecular weight = 80,000) with concentrated nitric acid (62 wt %) at 45°C and various reaction times

from 8 to 20 hours, and stabilization at  $-10^\circ\text{C}$  for 7 days. Subsequently, the products were then neutralized with a 1 wt % solution of sodium bicarbonate until the pH equalled 7. The neutralized solution was then dried in a vacuum oven at 70°C. A similar procedure for the preparation of PAN terpolymers, derived from its hydrolysis reaction, was disclosed in a patent.<sup>13</sup>

The gelation of the terpolymers prepared from the aforementioned procedure was achieved as follows: The obtained dried samples were dissolved into DMSO at 70°C and then mixed with  $\text{H}_2\text{O}$ . The final concentration was 1 g of polymers in 13 mL DMSO and 3 mL  $\text{H}_2\text{O}$ . The DMSO-water-polymer solutions were then cooled to room temperature and frozen at  $-10^\circ\text{C}$  for 12 h and thawed at 10°C for 12 h. This thermal cycling was repeated three times.

The contents of acrylamides and acrylic acids were determined by proton nuclear magnetic resonance (NMR) (Bruker AC-200) and base titration, respectively. The preparation and composition analysis were detailed in our previous publications.<sup>11,14</sup> Briefly speaking, the mole percentage of amide to three functional groups is the ratio of the NMR peak area at chemical shift equalling 6.7–6.8 ppm to that of methylene at 2.0 ppm (because each nitrile, carboxyl, or amide corresponds to a methylene). The base titration was carried out by titrating the xerogels (i.e., the completely dry gels) in DMSO solvent with 0.0482*N* aqueous KOH solution.

Considering PAN as a starting material for gel synthesis and its conversion into PAAm and PAA, we inferred that the PAN crystallites provide the physical crosslinking and the specific chemical interactions between PAA and PAAm function as another kind of crosslinking. However, due to the minor amount of PAA in copolymers (as shown in Table I), the latter crosslinking is of secondary importance as far as the elasticity of materials is concerned.

The chemical compositions and equilibrium water uptakes of seven samples with various hydrolysis times and the same stabilization, gelation, and freezing-thawing conditions are shown in Table I. The IR spectra, not shown here, exhibit the absorption of  $-\text{C}=\text{N}-$  group at  $1600\text{ cm}^{-1}$  and indicate the thermooxidation of PAN during acid hydrolysis. This degradation has been reported in the early literature.<sup>15,16</sup> The amount of imine is small, and cannot be determined on the proton-NMR spectra.<sup>11</sup> The xerogels look opaque and pale yellow due to their crystalline composition and degradation product. After the xerogels fully absorb the water, they appear transparent.

**Table I** Variation of Chemical Compositions with Hydrolysis Time for Polyacrylonitrile-Derived Terpolymer Gels

Sample Code <sup>a</sup>	TPH8	TPH10	TPH12	TPH14	TPH16	TPH18	TPH20
Nitrile content (mol %)	86.3	72.3	66.5	63.6	62.0	60.6	58.5
Amide content (mol %)	13.2	27.1	32.7	35.5	36.8	37.9	39.2
Acid content (mol %)	0.5	0.6	0.8	0.9	1.2	1.5	2.3
Water uptake (%) <sup>b</sup>	86.0	81.0	76.0	77.5	87.0	95.2	98.0

<sup>a</sup> The numbers in sample code represent the hydrolysis time in hours.

<sup>b</sup> (water weight)/(hydrogel weight + water weight) at 25°C.

The water uptake was obtained with a precision balance, with an accuracy to 0.0001 g. The hydrogel equilibrium water content (HEWC) data in Table I have a maximum deviation of 2%. Referring to Table I, the mol % of hydrophobic AN ranges from 59 to 86, and AAM from 13 to 39. It should be noted that the samples water contents first decrease and then increase with the increasing hydrolysis times. At the lower end of the acid/amide content, the larger amide content may lead to greater heterogeneity or crosslinking density. On the other end of the amide/acid content, the increasing acid results in more network defects or the transition layer between the acrylonitrile-rich phase and the acrylamide-rich phase. This argument has been proposed to explain the effects of chemical compositions and temperature on the hydration of this series of materials.<sup>12</sup> In addition, acid and amide contents monotonously increase with the hydrolysis time.

For comparison purposes, the chemically cross-linked PHEMA with water uptake amounting to 39 wt %, supplied by Oxlex Corp. (Hsinchu, Taiwan), was used in the contact angle measurement.

### Contact Angle Measurement and Calculation of Surface Energies

A technique for the measurement of contact angle in the aqueous phase, first described by Hamilton,<sup>17</sup> was used in this work. A similar technique was used by Lelah and colleagues.<sup>18</sup> A contact angle goniometer (FACE CA-D, Kyowa, Inc., Japan) was operated, using the injected *n*-octane drop and air bubble (0.2 cm diameter) suspended in water and in contact with gel samples situated on the elevated level. The contact angle between the gel and bubble/drop was determined at 25°C.

The surface free energy of hydrogel in air ( $\gamma_{sv}$ ), interfacial free energy between hydrogel and water ( $\gamma_{sw}$ ), polar interaction energy at hydrogel–water interface ( $I_{sw}$ ), polar component of surface energy of hydrogel ( $\gamma_{sv}^p$ ), and dispersion component of surface energy of hydrogel ( $\gamma_{sv}^d$ ) were obtained from contact angle data with air and *n*-octane, via the quantitative relationships proposed by Andrade and associates,<sup>4</sup> Fowkes,<sup>19</sup> and Tamai and colleagues.<sup>20</sup> The steps are briefly mentioned as follows:

(a) The measured contact angle of the air bubble with gels in water ( $\theta_1$ , in degree) is related to  $\gamma_{sv}$  and  $\gamma_{sw}$  via the Laplace–Young equation:

$$\gamma_{sv} - \gamma_{sw} = \gamma_{wv} \cos(\pi - \theta_1) \quad (1)$$

where  $\gamma_{wv}$  = energy at water–air interface = 72.1 erg/cm<sup>2</sup> at 25°C.

(b) The interfacial interaction energy,  $I_{sw}$ , is related to the contact angle for gel–normal octane in water environment,  $\theta_2$ , by

$$I_{sw} = \gamma'_{wv} - \gamma_{ov} - \gamma_{ow} \cos \theta_2 \quad (2)$$

where  $\gamma'_{wv}$  = surface tension of water saturated with *n*-octane, and is approximately numerically equal to  $\gamma_{wv}$ ;  $\gamma_{ov}$  = surface tension of octane, which is approximately equal to the dispersion component of surface tension of *n*-octane ( $\gamma_{ov}^d$ ) = 21.6 erg/cm<sup>2</sup> at 25°C; and  $\gamma_{ow}$  = interfacial energy at octane–water, approximately equal to the polar component of surface tension of water with a value of 50.5 erg/cm<sup>2</sup>, as referred to.<sup>4,5</sup>

(c) The above two equations, in combination with the following two expressions, lead to the  $\gamma_{sv}^d$ , the dispersion component of interfacial energy of gel–water, and  $\gamma_{sv}^p$ , the polar component:

$$\gamma_{sv}^d = \left[ \frac{(\gamma_{sv} - \gamma_{sw}) - I_{sw} + \gamma_{wv}}{2(\gamma_{wv}^d)^{1/2}} \right]^2 \quad (3)$$

$$\gamma_{sv}^p = I_{sw}^2 / (4\gamma_{wv}^p) \quad (4)$$

where  $\gamma_{wv}^p$  = polar component of surface tension for water = 51 erg/cm<sup>2</sup>.

(d) Then  $\gamma_{sv}$  is given by the sum of  $\gamma_{sv}^d$  and  $\gamma_{sv}^p$ , and  $\gamma_{sw}$  is obtained by eq. (1).

If we measure the contact angle of the water drop with the hydrogel in air, the following Laplace–Young equation, similar to eq. (1), is valid:

$$\gamma_{sv} - \gamma_{sw} = \gamma_{wv} \cos \alpha_1 \quad (1')$$

where  $\alpha_1$  is the contact angle.

If we measure the contact angle of the water drop with the hydrogel in *n*-octane (density of water > density of *n*-octane), we have:

$$\gamma_{so} - \gamma_{sw} = \gamma_{ow} \cos \alpha_2 \quad (2')$$

or equivalently:

$$I_{sw} = \gamma_{wv} - \gamma_{ov} - \gamma_{ow} \cos \alpha_2 \quad (2'')$$

After examining the similarity between eq. (1) and (1'), and between (2) and (2'), it is clear that contact angle data from the air bubble and octane drop in water suffice to yield calculated interfacial energy and interfacial interaction energy.

### Measurement of Equilibrium Adsorption of BSA onto Gels

BSA solutions of various concentrations, prepared by mixing BSA standard solution (Pierce, concentration = 2 mg/mL) and phosphate buffer solution (PBS) consisting of 0.5 M Na<sub>2</sub>HPO<sub>4</sub> (aq) and 0.125 M KH<sub>2</sub>PO<sub>4</sub> (aq), were used for calibration. One milliliter of BSA solution and 20 mL of reagent (Pierce) consisting of bicinchonic acid (BCA), sodium salt, and copper ion in solution, were reacted for 30 min at 60°C. BSA was converted to biuret under the basic conditions, and then the Cu<sup>+2</sup> ion was reduced to Cu<sup>+1</sup>, which led to the coordination with nitrogen atoms in bicinchonate ions.

The product of the resulting reaction, a blue-color complex, analyzed by an ultraviolet–visible spectrometer (UV/VIS Spectronic 1201, Milton Roy), showed a sharp peak at wavelength equal to 562 nm. The peak height or spectral absorbance was used to determine the BSA concentration in solution. The

above procedure was also referred to by Wiechelmann and colleagues.<sup>21</sup>

The hydrogel samples (surface area = 30 to 50 cm<sup>2</sup>) were placed in a petri dish, filled with 25 mL BSA solution (concentration = 60 μg/mL), for a preset time. BSA in the residue solution was then treated with the assay reagent, and the protein concentration (BSA concentration = 5 to 250 μg/mL) was determined with UV/VIS spectrometry in conjunction with the calibration curve for the UV absorbance–BSA concentration relationship. The amount of BSA adsorbed onto gels was the difference between the BSA amount in the original solution and that in the residue solutions in contact with gels. The calculated specific adsorption is based on the visually observed area of the flattened surface of the swollen gels.

## RESULTS AND DISCUSSION

### Surface Energetics of Hydrogels

Optical photographs for the suspended *n*-octane drop in contact with sample TPH20 (hydrolysis time = 20 h) and PHEMA in the water are depicted in Figures 1(a) and 1(b), respectively. TPH20 (water absorption = 98%) clearly shows less surface wetability by non-polar octane than does PHEMA (water absorption = 39%). A similar trend for the contact angle of the air bubble with P(AN–AAM–AA) and PHEMA is observed in Figures 2(a) and 2(b), in which the P(AN–AAM–AA) gel shows a greater contact angle ( $\theta$ ) than does PHEMA.

To ascertain if the above contact angle readings are for drops/bubbles in thermodynamic equilibrium with hydrogel surface, the contact angles for *n*-octane with samples TPH8, 12, 16, and 20 were measured against contact time, as shown in Figure 3. It convinced us that the contact angle measurements at contact time greater than 5 minutes yield the equilibrium data and the angles increase with the abundance of acrylamide or acrylic acid. Figure 4 depicts the time-independence of contact angles for air bubble with samples TPH8, 12, 16, and 20, wherein the contact angle decreases with the increasing contents of acrylamide and/or acrylic acid. Figure 5 shows the dispersion component of surface tension for gels in water (curve A), polar component of surface tension for hydrogels in air (curve B), total surface tension (curve C), and interaction energy between gel and water (curve D), using contact angle data and equations (2) to (4). Both the polar component of surface energy and the gel–water in-

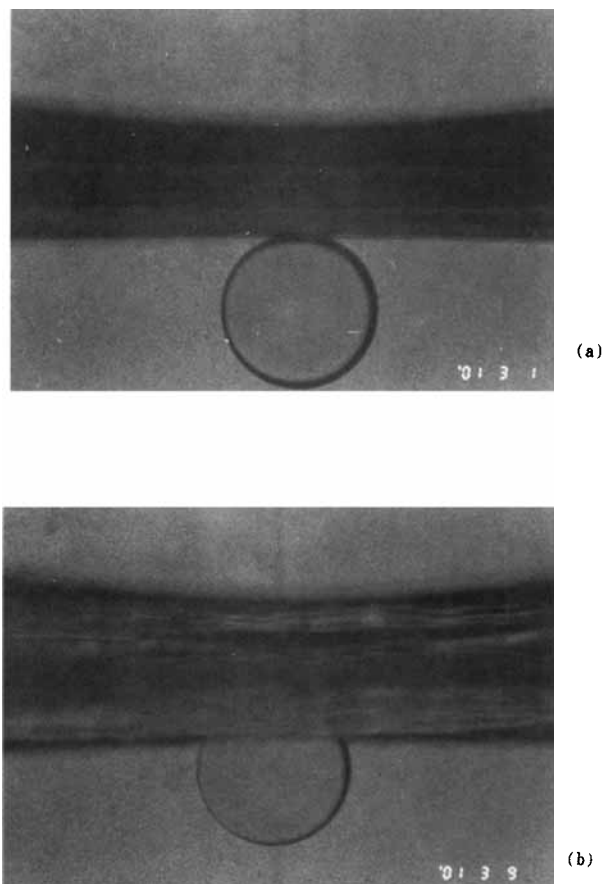


**Figure 1** Optical photography of a sessile *n*-octane drop in contact with the hydrogels (appearing as the shadowed membranes in photographs) in water: (a) P(AN-AAm-AA), TPH20; (b) PHEMA. The contact angle (always greater than 90°) is determined by the horizontal line along the gel membrane and the tangent line to the drop at the contact point between drop and gel.

teraction increase with the hydrolysis time, whereas the surface tension of hydrogels in air was affected by the hydrolysis in an opposite way. This implies that the surface polarity of hydrogels and their interfacial interaction energy with water increase with AAm-AA content in gels as indicated in Table I, regardless of the non-monotonous variation of water absorption with chemical composition. It should be noted that the total surface tension of gels decreases with the amount of hydrophilic components. The surface tension of solid polymers at room temperature is usually below 70 dyn/cm, and that of gels (water-polymer mixtures) below 72 dyn/cm (surface tension of water) sounds reasonable.

Figure 6 shows the interfacial energy between hydrogel and water ( $\gamma_{sw}$ ) as a function of hydrolysis time for gel preparation, which exhibits a minimal

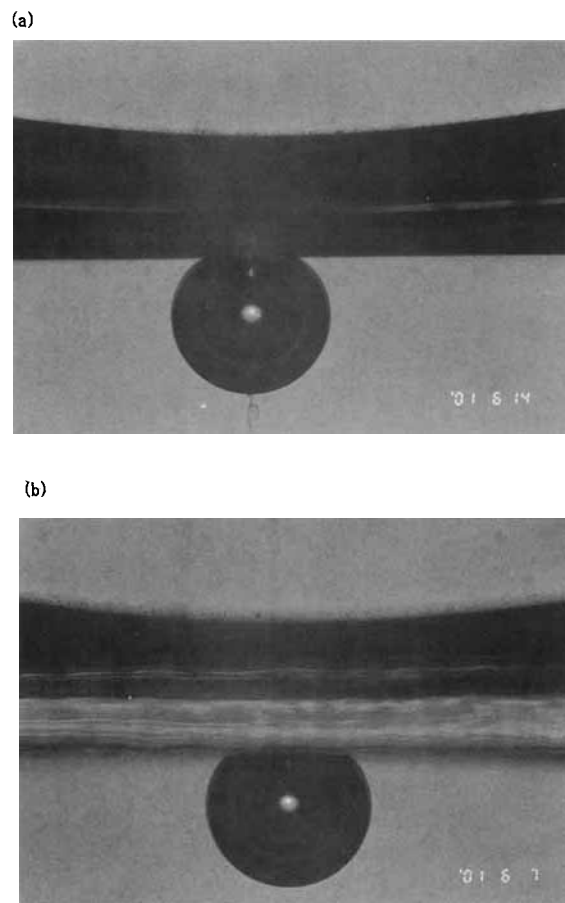


**Figure 2** Optical photography of an air bubble in contact with the hydrogel in water: (a) P(AN-AAm-AA), TPH16; (b) PHEMA.

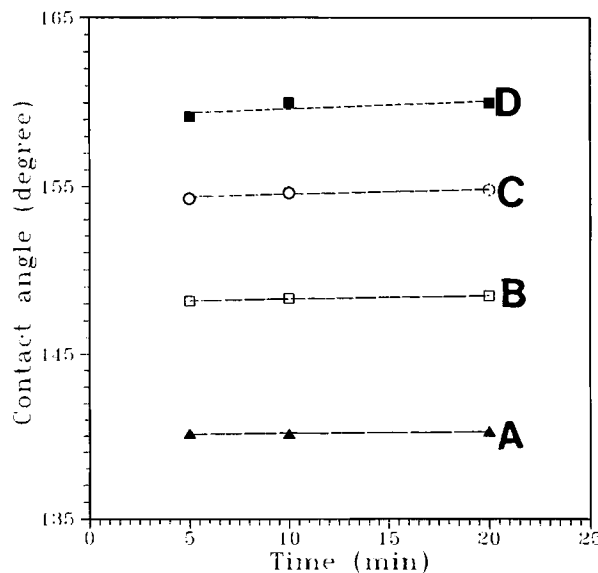


**Figure 3** Octane-gel-water contact angle versus contact time for samples with various hydrolysis times: (A) TPH8 (▲); (B) TPH12 (□); (C) TPH16 (○); (D) TPH20 (■).

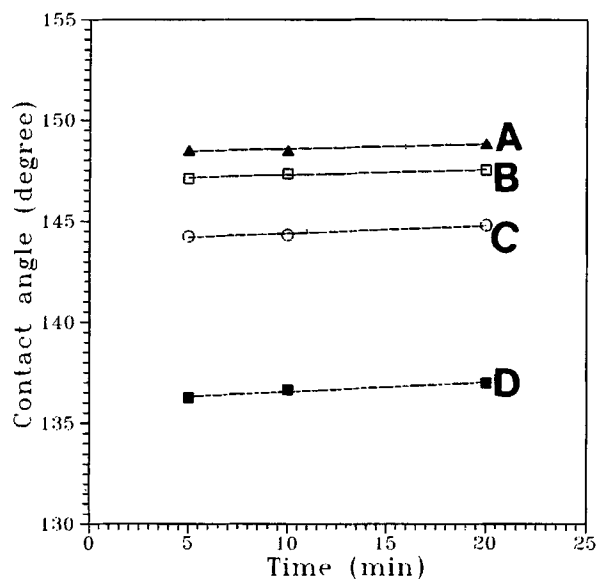


**Figure 4** Air-gel-water contact angle versus contact time for samples with various hydrolysis times: (A) TPH8 (▲); (B) TPH12 (□); (C) TPH16 (○); (D) TPH20 (■).

interfacial energy for TPH12 possessing the least water absorption among all samples investigated. Another way to characterize such an ionized interface of gels in the aqueous environment is to measure the interfacial or zeta potential.<sup>22</sup>

### BSA Adsorption onto Various Gels

The determination of the amount of BSA adsorption on gels relies on the sensitivity and accuracy of the quantitative analysis of the protein amount in albumin solutions with the aid of BCA assay. The calibration curves for such an analysis show the linear relationship between the absorbance of albumin solutions at wavelength equal to 562 nm and the concentration of albumin in solutions. Adsorption kinetics for BSA onto gels TPH8, 12, and 20 are presented in Figure 7. Each data point involves the triplicate run, having the maximum relative deviation of 11%. The adsorption processes for all samples reach the equilibrium states at the contact times for BSA and gels greater than 3 h, although the adsorption for TPH8 is the fastest to reach equilibrium. In addition, the affinity at initial adsorption stage and the saturation amount of BSA at gel-water interface is greater for gels with more surface polarity, as indicated in Figure 5. It should be mentioned that the albumin adsorption onto gels in dilute protein solution is not a simple Langmuir monolayer adsorption, because:

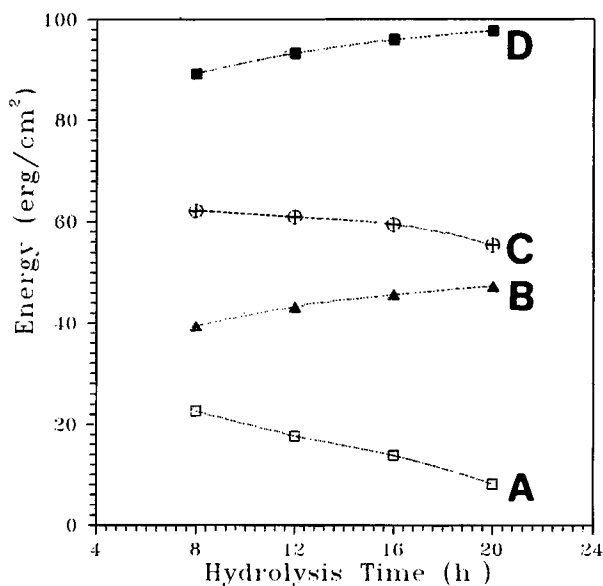


**Figure 5** Various surface/interfacial energy of hydrogels versus hydrolysis time during gel preparation: (A) dispersion component of surface tension of hydrogels in air,  $\gamma_{sv}^d$ ; (B) polar component of surface tension of hydrogels,  $\gamma_{sv}^p$ ; (C) total surface tension,  $\gamma_{sv}$ ; (D) polar interactions at hydrogel-water interface,  $I_{sw}$ .

1. several types of sites (i.e., multicomponent compositions and voids) exist;
2. there is irreversible adsorption for protein; and
3. more than one molecule may be adsorbed per site (i.e., multilayer adsorption).<sup>23</sup>

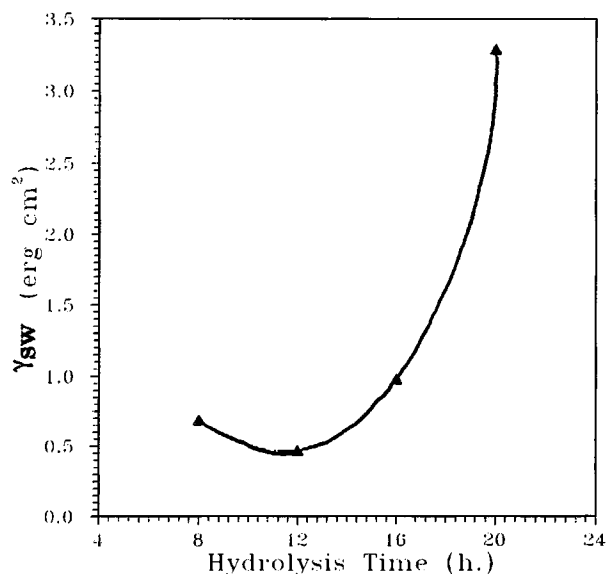


**Figure 6** Relationship of the hydrogel-water interfacial energy ( $\gamma_{sw}$ ) versus hydrolysis time of samples during preparation.

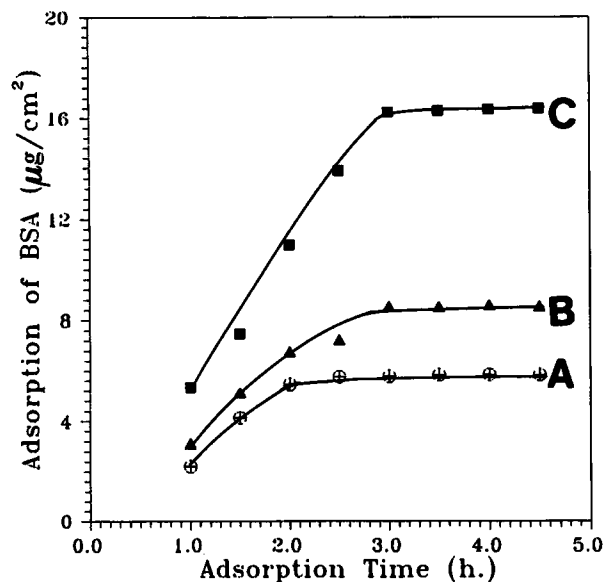


**Figure 7** BSA adsorption versus contact time for various samples: (A) TPH8 (hydrolysis time = 8 h); (B) TPH12; (C) TPH20. BSA conc. = 60  $\mu\text{g}/\text{mL}$ .

Figure 8 shows a linear relationship between equilibrium adsorption at 3-hour contact time versus the amount of acid groups in the bulk of seven samples. A similar plot of equilibrium adsorption against amide composition has been obtained but is not shown here for the sake of brevity. Castillo and colleagues<sup>8</sup> found that the bonding is formed between carboxyl groups in polymers and amine groups in proteins as detected by infrared spectroscopy, and such specific interactions account for the irreversible protein adsorption. Such a linear correlation in Figure 8 may imply the specific interactions occurring to gel-protein pairs.

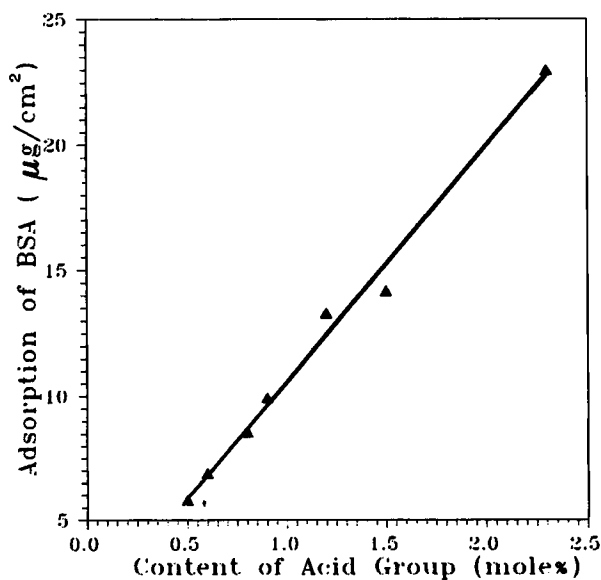
#### Correlation between BSA Adsorption and Interfacial/Bulk Properties

Figure 9 shows a rather empirical correlation between the apparent adsorption of protein and the polar component of surface tension of gels ( $\gamma_{sv}^p$ ), in which the higher surface polarity of gel in air leads to the greater adsorption. The amount of protein adsorption consists of multilayer surface adsorption and retention in pores. Figure 9 shows that the outcome of a complex process is empirically correlatable with surface polarity of gels. It implies that the initial interactions between protein and gel surface, controlled by the gel polarity, dominate the overall adsorption. Moreover, it should be emphasized that there is also a monotonous functional relationship

between the BSA adsorption and the polar interfacial interaction for gel and water by combining the curve D of Figures 5 and 8. It is therefore visualized that a monotonous relationship exists between interfacial composition of gels in water and the composition of the bulk. The relationship of BSA adsorption onto a variety of moderately hydrophilic polyoxyethylene/poly(L-lactide)/polyoxyethylene triblock copolymers against their surface polarity in air was found to be a decreasing function due to the hydrophobic interactions between polymers and BSA.<sup>24</sup> The different trend for protein adsorption, as exhibited by P(AN-AAm-AA) gel and the aforementioned polyetheresters, respectively, is partly attributed to the interfacial interactions between material and protein.

By taking into account the isoelectric point ( $PI$ ) of BSA ( $PI = 4.9$ ), BSA in the solution at pH 7.4 is negatively charged. At pH 7.4, the imidazolium groups of histidine of albumin have been partially titrated. The carboxyl groups in gels are bonded with amine groups in albumin. Subsequently, the albumin adsorbed onto negatively ionized gels may lead to the negative total charge of adsorbate-protein. However, a monotonous relationship between the BSA adsorption and gel-water interfacial energy cannot be obtained by cross-plotting Figures 5 and 9.

It is natural to assume that the outer molecular layer of hydrogels, placed in the air environment,



**Figure 8** Linear relationship of the amount of BSA adsorption onto gels versus the mole percentage of acid groups in the hydrogel bulk at adsorption time equal to 3 h.

may undergo restructuring once it contacts water. Although the bulk compositions in gels are given in Table I, the surface compositions of functional groups of multicomponent gels in air remain unanswered. To further demonstrate the role of water content in BSA adsorption, the BSA adsorption against the reciprocal of water content (or roughly the reciprocal of the percentage of void space occupied by water to the overall gel volume) is plotted in Figure 10. The lower portion of two distinct regimes in this plot is for TPH8, TPH10, and TPH12, indicating that lower water absorption leads to higher BSA adsorption. The increasing pore volume on the lower portion "prohibits" the protein adsorption. It can be assumed that the apparent overall adsorption involves both albumin adsorption at gel-water interface and albumin retention in pores. The latter step is the outcome of protein diffusion into swelling-controlled pores with size in the order of several hundred angstroms. Although we do not have the pore-size data from the permeation test using macromolecules, it is plausible to use the water absorption to characterize the expansion of swollen networks. As a consequence, the adsorption kinetics in the initial stage presented in Figure 7 is influenced by the albumin diffusion in the solution through the boundary layer and the diffusion in pores. The interfacial adsorption is predominantly determined by the outer layer composition of hydrogels, and the upper portion on Figure 10 indicates that the increasing acrylic acid composition of outlayer of gels favors the interactions. This is also the case for pro-

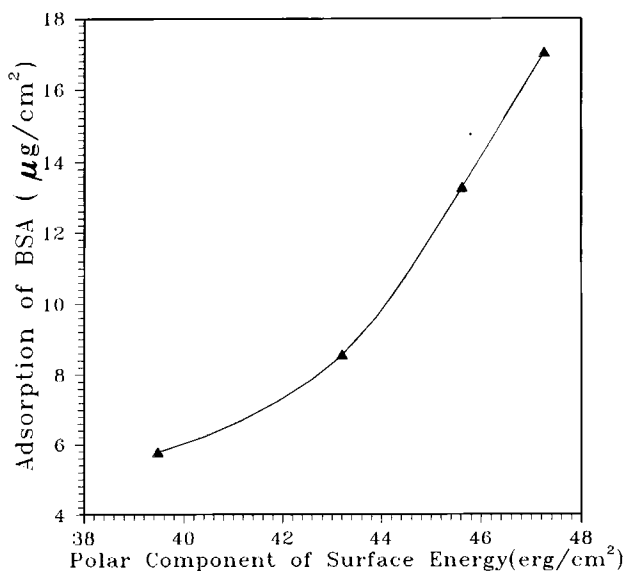


**Figure 9** Correlation of BSA adsorption with the polar component of the surface tension of hydrogels in air.

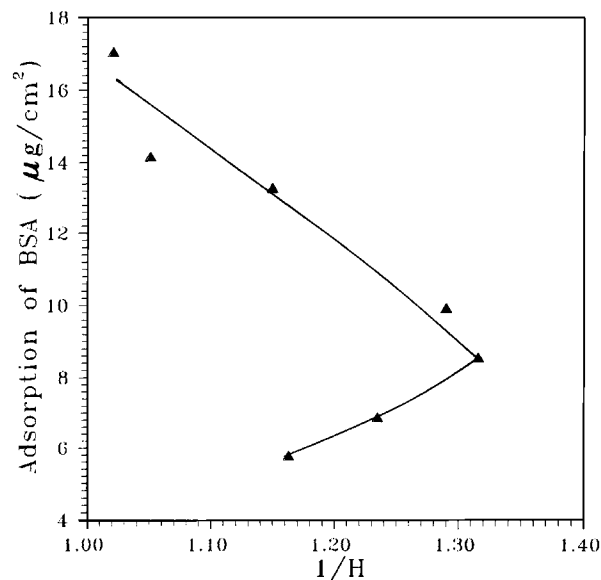


**Figure 10** Correlation of BSA adsorption with the reciprocal of water absorption at 23°C, where  $H$  is the wt % of water in hydrogels. Please note the two distinct regions on this curve.

tein adsorption on to ionic P(HEMA/MAA) gels. The lower portion on Figure 10 represents the situation similar to the neutral PHEMA and its copolymer gels, in spite of the possible different modes of protein-substrate interactions for P(AN-AAm-AA) and PHEMA gels, respectively. In PHEMA/albumin systems, the hydrophobic interactions between gels and protein and protein diffusion into pores affect the amount of protein adsorption.

The complexation between gel and protein is certainly determined by an abundance of PAA in the 0.5 to 2.3 mol % range. This minor amount of acid and the PAN crystallites acting as the reinforcement element of mechanical strength make the swelling or deswelling due to gel-protein interactions not observable with the length measurement.

The phase behavior of multiphase/multicomponent gels and its influence on the chemical composition of gel surface in the air is open to question. Nevertheless, it is proposed that the gel with minimal water absorption, i.e., TPH12, has maximum crosslink density or microphase clustering and contains the lowest amount of non-bound water in light of the three-water-state model. This point regarding the gel structure is discussed elsewhere.<sup>12</sup> In that paper, the bound water (in grams of water per gram of dry polymer) in hydrogels, rather than the unbound or total absorbed water in gels, was found to increase with the contents of amide/acid. The water in bound state (in the immediate vicinity of the



polymer) may be disturbed or reoriented during protein-gel interactions.

## CONCLUSIONS

This paper addresses the relationships among water absorption in, surface/interfacial energetics of, and protein adsorption onto a series of multicomponent ionic gels which possess the dual nature of neutral and ionic species. The surface tension of hydrogels in air environment and its contribution from dipole-dipole interactions in gel bulk are merely dependent on the strong polar functional groups in the xerogels.

The BSA adsorption onto the multicomponent ionic gels seems more complex than structurally simple gels. The BSA adsorption of gels in the aqueous environment is correlated well with the abundance of functional groups such as amide and acids, and the resulting surface polarity in both air and water increases the BSA adsorption of gels in the aqueous environment. However, the effects of polymer swelling on protein adsorption exhibit in two opposite ways, depending on the range of the abundance of strong polar functional groups. At the lower side of the abundance of amide/acid, the phase separation behavior makes more water uptake in polymers disfavor the protein adsorption. On the other hand, the more hydrophilic compositions or water uptake favor the protein adsorption at higher contents of amide/acid. The hydrophilic amide and acid composition appearing on the gel-water interface is the predominant factor affecting the process of protein adsorption.

The authors would express their gratitude to the National Science Council, R. O. C., under a contract NSC-82-0405-E-011-039. The donation of commercially available PHEMA samples by Dr. Gregory C. Niu at Oxlex Corp. (Hsinchu, Taiwan) is also highly appreciated.

## REFERENCES

1. N. A. Peppas ed., *Hydrogels in Medicine and Pharmacy*, 3 volumes, CRC Press, Boca Raton, Florida, 1987.
2. R. S. Harland and R. E. Prudhomme, eds., *Polyelectrolyte Gels*, ACS Symp. Ser. 480, American Chemical Society, Washington, DC, 1992.
3. A. S. Hoffman, *J. Controlled Release*, **6**, 297 (1987).
4. J. D. Andrade, R. N. King, D. E. Gregonis, and D. L. Coleman, *J. Polym. Sci.: Polym. Symp.*, **66**, 313 (1979).
5. Y. C. Ko, B. D. Ratner, and A. S. Hoffman, *J. Colloid Interface Sci.*, **83**, 25 (1981).
6. T. A. Horbett and A. S. Hoffman, in *Applied Chemistry at Protein Interfaces*, R. E. Baier, ed., *Advances in Chemistry*, Vol. 145, American Chemical Society, 1975, p. 230.
7. P. K. Weatherby, T. A. Horbett, and A. S. Hoffman, *J. Bioeng.*, **1**, 395 (1977).
8. E. J. Castillo, J. L. Koenig, J. M. Anderson, and N. Jentoft, *Biomaterials*, **7**, 9 (1986).
9. Y. Sakurai, T. Akaike, K. Kataoka, and T. Okano, in *Biomedical Polymers*, E. P. Goldberg and A. Nakajima, eds., Academic Press, New York, 1980, p. 335.
10. M. Kumakura, M. Yoshida, and M. Asano, *J. Appl. Polym. Sci.*, **41**, 177 (1990).
11. D. S.-G. Hu and Y.-S. Lin, *Macromol. Chem. Phys. (Makromol. Chem.)*, to appear.
12. D. S. G. Hu and M. T. S. Lin, *Polymer*, to appear.
13. V. Stoy, A. Stoy, J. Prokop, R. Urbanova, and J. Kucera, U.S. Patent 3 948 870, 1976.
14. D. S. G. Hu and Y. S. Lin, *ACS Polymer Preprints*, **34** (1), 824 (1993).
15. W. J. Burlant and J. L. Parsons, *J. Polym. Sci.*, **22**, 249 (1956).
16. I. B. Klimenko, N. V. Platonova, V. I. Grachev, N. P. Gracheva, A. G. Khasbulatova, and L. M. Novichkova, *Polym. Sci. U.S.S.R.*, **24**, 1597 (1982).
17. W. C. Hamilton, *J. Colloid Interface Sci.*, **40**, 219 (1972).
18. M. D. Lelah, L. Lambrecht, B. R. Young, and S. L. Cooper, *J. Biomed. Mater. Res.*, **17**, 1 (1983).
19. F. M. Fowkes, *Ind. Eng. Chem.*, **56**, 40 (1964).
20. Y. Tamai, K. Makunchi, and M. Suzuki, *J. Phys. Chem.*, **71**, 4176 (1967).
21. K. Wiechelmann, R. Braun, and J. Fitzpatrick, *Anal. Biochem.*, **175**, 231 (1988).
22. G. Harkes, J. Dankert, and J. Feijen, *J. Biomater. Sci., Polym. Ed.*, **3**, 403 (1992).
23. A. Silberberg, in *Surface and Interfacial Aspects of Biomedical Polymers, Vol. 2: Protein Adsorption*, J. D. Andrade, ed., Plenum Press, New York, 1985, p. 321.
24. D. S.-G. Hu, H.-J. Liu, and I.-L. Pan, *J. Appl. Polym. Sci.*, **50**, 1391 (1993).

Received November 3, 1994

Accepted June 17, 1995